

C–H Activation

Rhoda-Electrocatalyzed Bimetallic C–H Oxygenation by Weak O-Coordination

Xuefeng Tan⁺, Leonardo Massignan⁺, Xiaoyan Hou, Johanna Frey, João C. A. Oliveira, Masoom Nasih Hussain, and Lutz Ackermann*

In memory of Professor Jean-Michel Savéant

Abstract: Rhodium-electrocatalyzed arene C–H oxygenation by weakly O-coordinating amides and ketones have been established by bimetallic electrocatalysis. Likewise, diverse dihydrooxazinones were selectively accessed by the judicious choice of current, enabling twofold C–H functionalization. Detailed mechanistic studies by experiment, mass spectroscopy and cyclovoltammetric analysis provided support for an unprecedented electrooxidation-induced C–H activation by a bimetallic rhodium catalysis manifold.

Introduction

During the past decade, transition metal-catalyzed C–H activation has been recognized as a transformative tool in molecular syntheses.^[1] Phenols featuring an *ortho*-substituted carbonyl group constitute important structural motifs of a diversity of bioactive molecules, ranging from natural products to drugs molecules.^[2] Transition metal-catalyzed C–H activation by weak chelation assistance provides a straightforward access to the assembly of phenols.^[3] Pioneering studies with palladium catalysis were accomplished by Dong^[4] and Rao.^[5] In the same year, our group reported sustainable ruthenium-catalyzed C–H oxygenations with a diverse range of weakly coordinating groups.^[6] In addition, considerable efforts have been devoted to the development of different metal catalysts, along with various oxidants.^[7] Despite indisputable advances, stoichiometric

How to cite: *Angew. Chem. Int. Ed.* **2021**, *60*, 13264–13270

International Edition: doi.org/10.1002/anie.202017359

German Edition: doi.org/10.1002/ange.202017359

amounts of strong chemical oxidants, such as (diacetoxyido)benzene and K₂S₂O₈, are required, which leads to undesired byproducts.

Electrochemical synthesis has undergone a renaissance in recent years towards environmentally-benign organic synthesis.^[8] Significant recent impetus was gained by the merger of electrocatalysis with oxidative C–H activation, thus avoiding the use of toxic and expensive metal oxidants.^[9] Although transition metal-catalyzed electrochemically C–H oxygenation have been recently realized,^[10] this mostly required strong *N*-coordination, such as bidentate quinolinyl amides or pyridines, while the very recently devised ruthenium catalysis needed rather costly aryl iodides as additional redox mediators, jeopardizing the inherent atom-economy.^[10a] In contrast, the redox direct—mediator-free—oxidation of homogeneous metal oxygenation catalysts at the anode surface typically called for a divided cell setup.^[10e–g] Within our program on electrochemical C–H activation,^[11] we have now devised mechanistically-distinct rhoda-electrocatalyzed C–H oxygenations of weakly-O-coordinating amides and ketones (Figure 1). Salient features of our findings include 1) undivided cell without redox mediator, 2) room temperature oxygenations, 3) electricity in lieu of strong oxidants, 4) high Faraday efficiency, 5) twofold electrochemical C–H functionalization towards dihydrooxazinones,^[12] and 6) detailed mechanistic support for a bimetallic electrocatalysis manifold.

[*] Dr. X. Tan,^[a] L. Massignan,^[a] X. Hou, Dr. J. Frey, Dr. J. C. A. Oliveira, M. N. Hussain, Prof. Dr. L. Ackermann

Institut für Organische und Biomolekulare Chemie, Georg-August-Universität Göttingen

Tammannstraße 2, 37077 Göttingen (Germany)

E-mail: Lutz.Ackermann@chemie.uni-goettingen.de

Prof. Dr. L. Ackermann

Wöhler Research Institute for Sustainable Chemistry, Georg-August-Universität Göttingen

Tammannstraße 2, 37077 Göttingen (Germany)

[†] These authors contributed equally to this work.

Supporting information and the ORCID identification number(s) for the author(s) of this article can be found under:

<https://doi.org/10.1002/anie.202017359>.

© 2021 The Authors. *Angewandte Chemie International Edition* published by Wiley-VCH GmbH. This is an open access article under the terms of the Creative Commons Attribution Non-Commercial License, which permits use, distribution and reproduction in any medium, provided the original work is properly cited and is not used for commercial purposes.

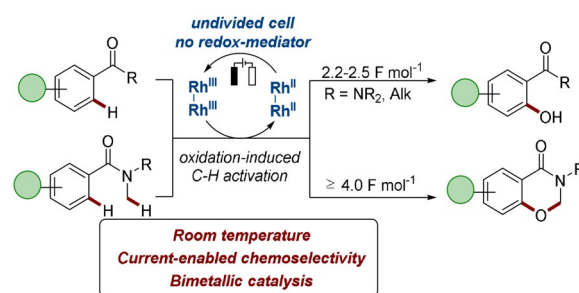
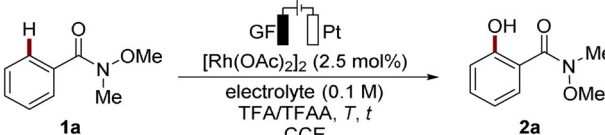


Figure 1. Rhoda-electrocatalyzed C–H oxygenation.

Results and Discussion

At the outset of our studies, various reaction conditions were explored for the envisioned redox-mediator-free, rhoda-electrocatalyzed C–H oxygenation of **1a** in an operationally

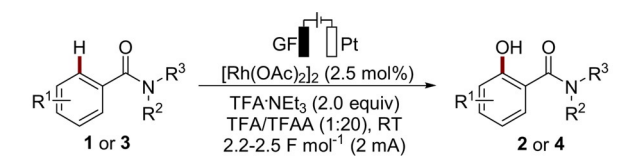
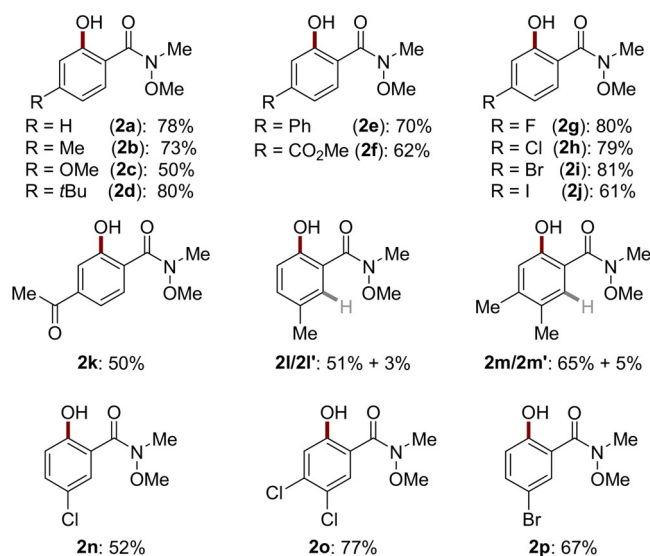
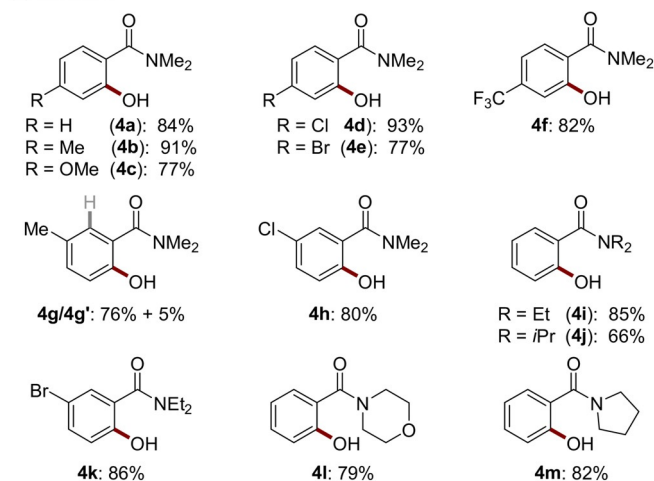
Table 1: Optimization of the rhoda-electrocatalyzed C–H oxygenation.^[a]


Entry	Electrolyte	TFA/TFAA	I [mA]	t [h]	T [°C]	Yield [%]
1	CF ₃ COONa	3:1	4	16	50	trace
2	LiClO ₄	3:1	4	16	50	24
3	<i>n</i> Bu ₄ NBF ₄	3:1	4	16	50	22
4	<i>n</i> Bu ₄ NPF ₆	3:1	4	16	50	28
5	<i>n</i> Bu ₄ NPF ₆	1:1	4	16	50	42
6	<i>n</i> Bu ₄ NPF ₆	1:1	4	16	RT	54
7	<i>n</i> Bu ₄ NPF ₆	1:2	4	16	RT	52
8	<i>n</i> Bu ₄ NPF ₆	1:3 ^[b]	4	16	RT	trace
9	<i>n</i> Bu ₄ NPF ₆	1:1	0	16	RT	ND
10	<i>n</i> Bu ₄ NPF ₆	1:1	4	16	RT	trace ^[c]
11	<i>n</i> Bu ₄ NPF ₆	1:1	4	16	RT	57 ^[d]
12	TFA·NEt ₃ ^[e]	1:20	4	8	RT	76 ^[d]
13	TFA·NEt ₃ ^[e]	1:20	2	15	RT	82 ^[d]
14	TFA·NEt ₃ ^[e]	1:20	2	15	RT	ND ^[f]
15	<i>n</i> Bu ₄ NPF ₆	3:1	4	16	50	28 ^[g]
16	TFA·NEt ₃ ^[e]	1:20	2	15	RT	52 ^[h]

[a] **1a** (0.5 mmol), [Rh(OAc)₂]₂ (2.5 mol%), electrolyte (0.10 M), TFA/TFAA, GF anode (10 mm × 10 mm × 6 mm), Pt cathode (10 mm × 15 mm × 0.125 mm). [b] Poor conductivity due to poor solubility of electrolyte. [c] Without [Rh(OAc)₂]₂. [d] Under N₂. [e] TFA·NEt₃ (0.33 M). [f] [RhCp*Cl₂]₂ or RhCl₃·3H₂O instead of [Rh(OAc)₂]₂ as the catalyst. [g] Ru(OAc)₂(*p*-cymene) (5 mol%) as the catalyst. [h] [Rh(OPiv)₂]₂ as the catalyst. Piv = pivalate.

simple undivided cell equipped with a graphite felt (GF) anode and a platinum cathode (Table 1 and Table S1 in the Supporting Information).^[13] Preliminary experimentation indicated that *n*Bu₄NPF₆ was the optimal additive (Table 1, Entries 1–4). Further studies revealed that the reaction was viable at ambient temperature (Entries 5–6) in a solvent mixture of trifluoroacetic acid (TFA) and trifluoroacetic anhydride (TFAA) (1:1) (Entries 6–8). Control experiments showed that both the rhodium catalyst and electricity were essential (Entries 9–11). During the optimization, we found that NEt₃ could significantly improve the conductivity (Table S1). Thus we employed easily available TFA·NEt₃ salt (Entry 12),^[14] enabling the use of a solvent mixture TFA/TFAA (1:20) without solubility or conductivity problems (Entries 12–13 vs. Entry 8). Here, the highest yield of 82% was obtained with 2 mA (Entry 13). Interestingly, while [Rh(OAc)₂]₂ showed high catalytic efficacy, the commonly used [RhCp*Cl₂]₂ or RhCl₃·3H₂O provided unsatisfactory results (Entry 14).

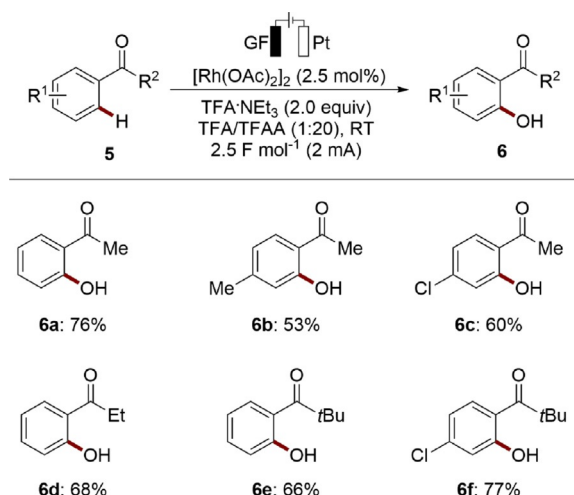
With the optimized reaction conditions in hand, we next examined the viable substrate scope of the rhodium-catalyzed electrochemical C–H oxygenation with various weakly coordinating Weinreb amides **1** (Scheme 1 a). Electron-rich as well as electron-deficient Weinreb amides **1a–1p** were amenable to the rhodium-catalyzed electrochemical catalysis. Notably, a diverse array of valuable functional groups, including ester (**2f**), halogen (**2g–2j**) and ketone (**2k**) groups, were tolerated by the electrocatalysis, highlighting a notable potential for further late-stage diversification. It is noteworthy that the

**(a) Weinreb amides 1****(b) amides 3****Scheme 1.** Rhoda-electrocatalyzed C–H oxygenation of amides **1** and **3**.

rhoda-electrocatalysis was not limited to Weinreb amides **1**. Indeed, differently substituted amides **3a–m** were also efficiently converted into the corresponding oxygenated amides **4a–m** with remarkable catalytic efficiency (Scheme 1 b).

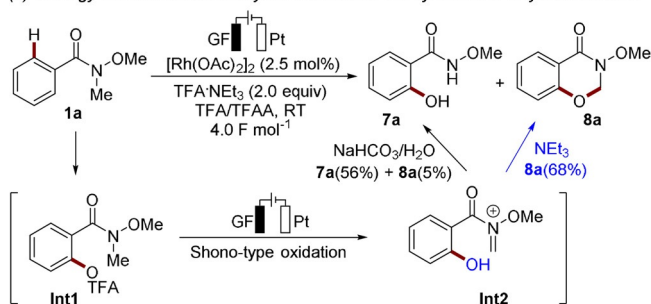
The outstanding robustness of the rhoda-electrocatalyzed C–H oxygenation was further highlighted by its ability to transform more challenging ketones **5** (Scheme 2).

During our optimization studies, small amounts of *N*-demethylation product **7a** could often be isolated (Scheme 3 a). Hence, we rationalized that it was formed through a cascade C–H oxygenation, along with Shono-type oxidation to generate **Int2**. Further experimentation at Q ≥ 4 F mol^{−1} revealed small amounts of an interesting dihydrooxazinone

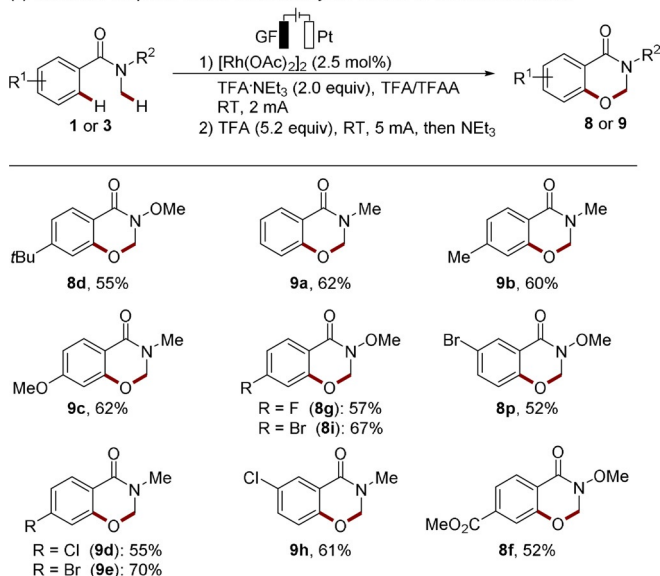


Scheme 2. Rhoda-electrocatalyzed C–H oxygenation of ketones **5**.

(a) Strategy of rhoda-electrocatalyzed cascade for the synthesis of dihydrooxazinone



(b) Substrate scope for rhoda-electrocatalyzed double C–H functionalization

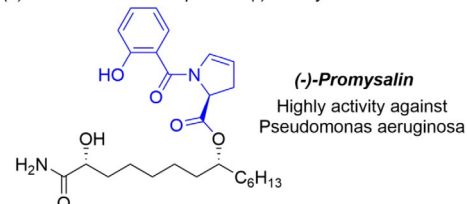


Scheme 3. Rhoda-electrocatalyzed cascade reaction for the synthesis of dihydrooxazinones.

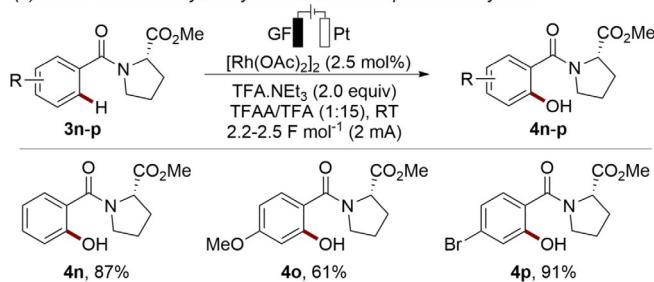
8a. Through rational design of the work up process with NEt₃ as non-nucleophilic base, **Int2** could be exclusively converted to the valuable dihydrooxazinone^[12] **8a** (Scheme 3a, blue

path). With the optimized reaction conditions, we explored the substrate scope of the rhoda-electrocatalyzed cascade reaction with diverse amides **1** and **3** to assemble various dihydrooxazinones **8** and **9** (Scheme 3b). The tolerance of ester (**8f**) and halogen (**8g**, **8i**, **8p**, **9d–e**, **9h**) substitute provides an invaluable asset in terms of late-stage modifications.

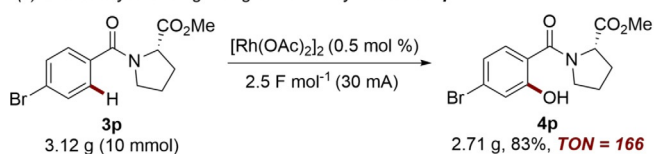
(a) Structure of natural product (–)-Promysalin



(b) Rhoda-electrocatalyzed synthesis of diverse proline-salicylates



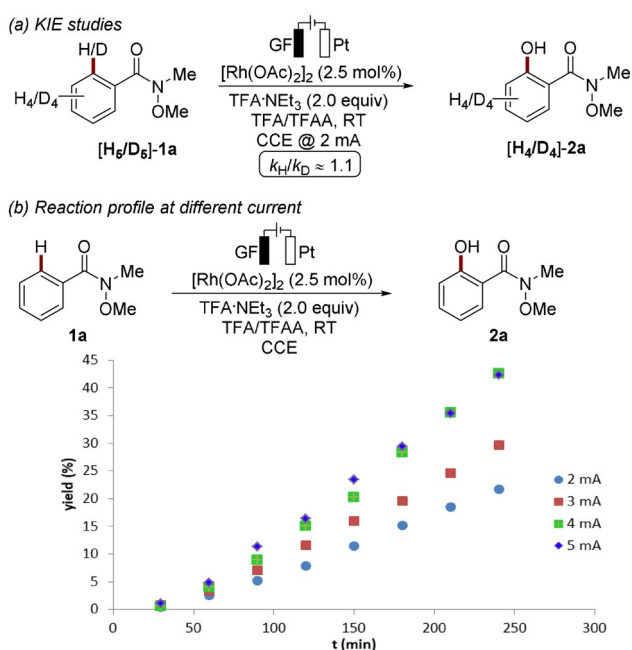
(c) Low catalyst loading and gram-scale synthesis of **4p**



Scheme 4. Application to the synthesis of the analogous fragments of Promysalin.

Promysalin is a *Pseudomonas* secondary metabolite that exhibits narrow-spectrum antibacterial activity, originally isolated from the rhizosphere (Scheme 4a).^[15] In 2016, Wuest reported the total synthesis of Promysalin analogues.^[15b] The key proline-salicylate fragment in Promysalin inspired us to apply our rhoda-electrocatalyzed C–H oxygenation to the synthesis of various substituted proline-salicylates (**4n–p**) without any protection and deprotection of the phenol motif (Scheme 4b). Next, we studied the efficiency of the catalysis with bromo analog **3p** through the gram-scale synthesis with only 0.5 mol % of [Rh(OAc)₂]₂ with a turnover number of 166 based on the rhodium-dimer, along with the solvent TFAA being recovered by simple distillation, highlighting the practical potential of this catalysis (Scheme 4c).

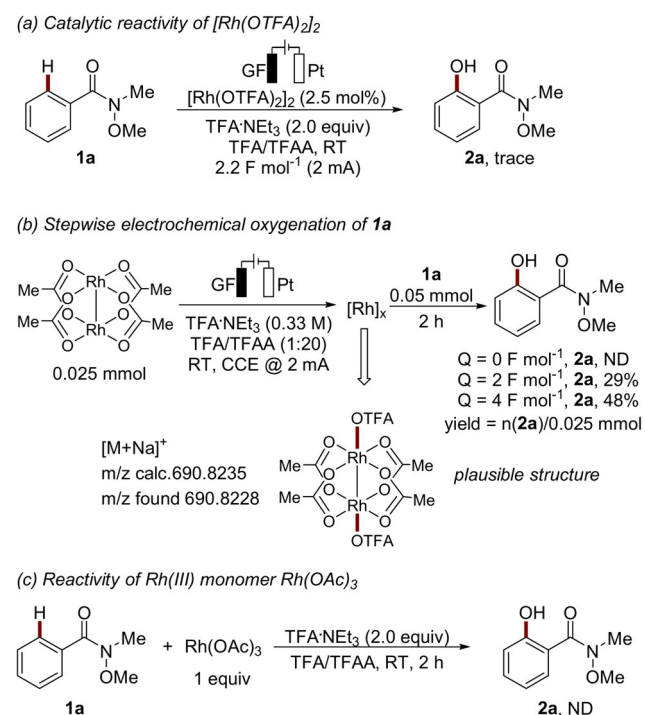
Given the versatility of the redox mediator-free electrochemical C–H oxygenation, we became attracted to probing its mode of action. Reactions conducted with isotopically labeled [D]₁-TFA did not lead to any H/D scrambling.^[13] Kinetic studies provided strong support for a fast C–H metalation with a minor kinetic isotope effect (KIE) of *k*_H/*k*_D ≈ 1.1 (Scheme 5a). Then, we explored the current dependence of the performance within a range from 2.0 to 5.0 mA,



Scheme 5. Key mechanistic experiments.

being indicative of a turnover-limiting electron transfer step in the current region of 2.0–4.0 mA (Scheme 5b). Beyond 4.0 mA the reaction rate did not increase significantly, being suggestive of a switch in the turnover-limiting step.

Next, we turned our attention to investigate the ligand exchange effect at rhodium. Somewhat surprisingly, $[\text{Rh}(\text{OTFA})_2]_2$ did not show any catalytic reactivity for this

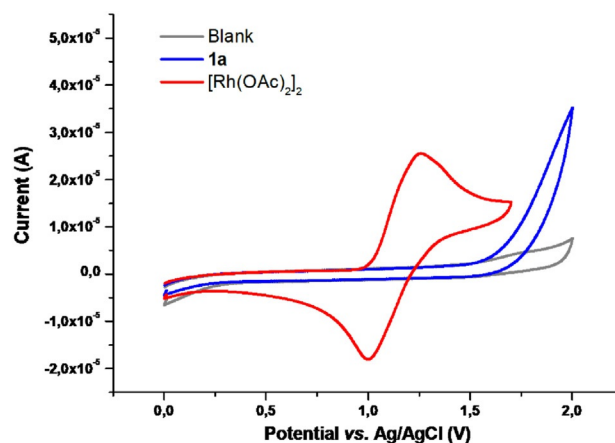


Scheme 6. Mechanistic studies on rhoda-electrocatalyzed oxygenation.

electrochemical catalysis (Scheme 6a). Mass spectroscopy studies revealed a rapid -OAc/-OTFA exchange in the solvent mixture TFA/TFAA (1:1), while in TFA/TFAA (1:20) this exchange was slow,^[13] which may be caused by the low concentration of available TFA. These observations are matched with the low catalytic activity in TFA/TFAA (1:1) (Table 1), suggesting the ligand exchange to be harmful to the catalyst activity. While stepwise electrochemical oxygenation delineated an oxidation-induced C–H activation and oxygenation, mass spectroscopic analysis of the electrolyzed mixture showed a plausible active intermediate $[\text{Rh}(\text{OAc})_2(\text{OTFA})]_2$, highlighting the dimeric form of the catalyst (Scheme 6b). This was further experimentally supported by the inactivity of the monomeric $\text{Rh}(\text{OAc})_3$ (Scheme 6c).

Furthermore, we probed an electrochemical oxidation-induced C–H activation by means of cyclic voltammetric analysis (Figure 2). First, the oxidation potential of amide

(a) Oxidation potential comparison of $[\text{Rh}(\text{OAc})_2]_2$ and **1a**



(b) Cyclic voltammetry of $[\text{Rh}(\text{OAc})_2]_2$ in TFA/TFAA mixture

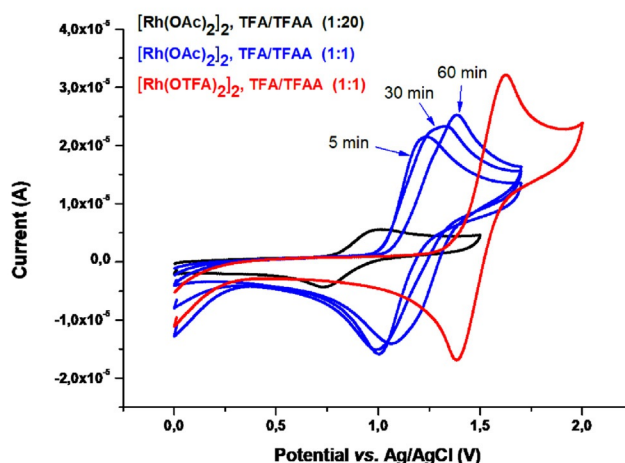


Figure 2. Cyclic voltammetry measurements in TFA/TFAA with 0.15 M TFA·NEt₃ and 5 mM substrate at RT with a scan rate of 100 mV s⁻¹: (a) in TFA/TFAA (1:1); (b) dark, $[\text{Rh}(\text{OAc})_2]_2$ in TFA/TFAA (1:20), stirred 10 min, poor solubility; blue, $[\text{Rh}(\text{OAc})_2]_2$ in TFA/TFAA (1:1), measured at stirring 5, 30 and 60 min; red, $[\text{Rh}(\text{OTFA})_2]_2$ in TFA/TFAA (1:1).

1a was higher than $[\text{Rh}(\text{OAc})_2]_2$ in TFA/TFAA (1:1), suggesting an oxidation-induced C–H activation regime (Figure 2a). In TFA/TFAA (1:20), $[\text{Rh}(\text{OAc})_2]_2$ featured an onset potential of $E_{\text{onset}} = 0.8$ V vs. Ag/AgCl with low current, due to the poor solubility of $[\text{Rh}(\text{OAc})_2]_2$ (Figure 2b, dark). In TFA/TFAA (1:1), the oxidation peak shifts to higher oxidation potentials, this shift is likely caused by gradually -OAc/-OTFA ligand exchange, implying the more -OTFA substituents on rhodium, the higher oxidation potential exhibited (Figure 2b, blue). In line with this observation, $[\text{Rh}(\text{OTFA})_2]_2$ revealed a high onset potential of $E_{\text{onset}} = 1.3$ V vs. Ag/AgCl, which further rationalized as to why $[\text{Rh}(\text{OTFA})_2]_2$ was not catalytically competent (Figure 2b, red).

Likewise, the catalyst's mode of action was investigated by means of DFT studies at the B3LYP-D4/6-311++G**,Rh/SDD+SMD(DCE)//B3LYP-D3/6-31G**,Rh/SDD level of theory.^[13] Thus, several bimetallic rhodium complexes were probed, namely monocationic (Figure S9) or dicationic (Figure 3) $\text{Rh}^{\text{III}}\text{-Rh}^{\text{III}}$ as well as monocationic $\text{Rh}^{\text{II}}\text{-Rh}^{\text{III}}$ (Fig-

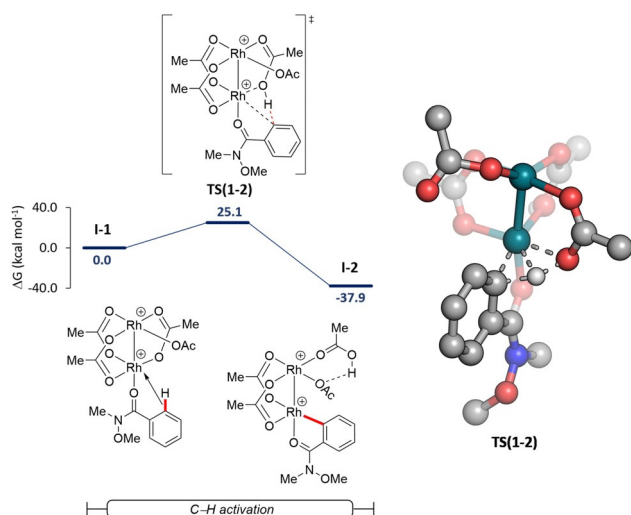


Figure 3. Computed relative Gibbs free energies ($\Delta G_{298,15}$) in kcal mol^{-1} for the C–H activation elementary step at the B3LYP-D4/6-311++G**,Rh/SDD+SMD(DCE)//B3LYP-D3/6-31G**,Rh/SDD level of theory for a dicationic $\text{Rh}^{\text{III}}\text{-Rh}^{\text{III}}$ complex. In the computed transition state structure, non-relevant hydrogens were omitted for clarity.

ure S11). According to our findings, a C–H rhodation via dicationic $\text{Rh}^{\text{III}}\text{-Rh}^{\text{III}}$ complex was identified as the most plausible pathway with an activation barrier of 25.1 kcal mol^{-1} .

On the basis of our mechanistic studies, we propose a plausible catalytic cycle to be initiated by facile electrochemical oxidation of $[\text{Rh}(\text{OAc})_2]_2$ to generate the rhodium(III)-rhodium(II) species **10** (Figure 4). A subsequent anodic oxidation generates the catalytically competent bimetallic rhodium(III) species **11**. Notably, the bimetallic nature of the electrocatalysis allows for effective direct oxidations in the absence of a redox mediator. Then, isomerization and substrate coordination occur to deliver intermediate **12**.

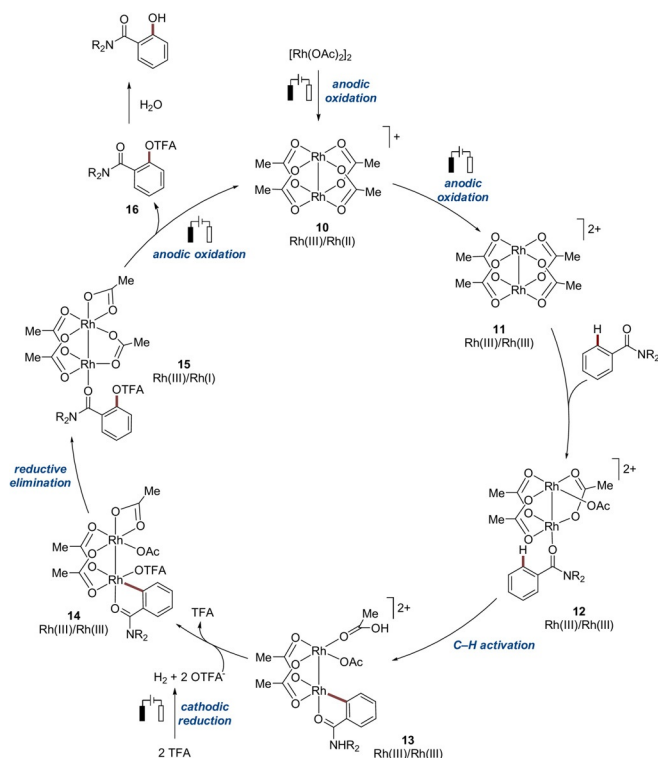


Figure 4. Proposed catalytic cycle.

Thereafter, the high-valent bimetallic rhodium-induced C–H activation takes place, while, reductive elimination and decoordination deliver the trifluoroacetate ester **16**. Finally, anodic oxidation regenerates the catalyst **10**, with an alternative two-electron oxidation pathway being depicted in Scheme S12.^[13]

Conclusion

In conclusion, we have reported on mechanistically-distinct rhoda-electrocatalysis for C–H oxygenations of synthetically useful amides and ketones by challenging weak *O*-coordination. In an undivided cell, an easily accessible ionic liquid and mild reaction conditions set the stage for an operationally-friendly C–H oxygenation in the absence of redox mediators. By adjusting the current, valuable dihydrooxazinones could be selectively assembled by double C–H functionalization. The application to the late-stage assembly of Promysalin analogue fragments with a low catalyst loading, as well as gram-scale bimetallic electrocatalysis accounts for the considerable practical potential. Detailed mechanistic studies revealed an oxidation-induced C–H activation by a bimetallic rhodium catalysis manifold.

Acknowledgements

Generous support by the DFG (Gottfried-Wilhelm-Leibniz award to L.A.) and the CSC (fellowship to XYH) is gratefully

acknowledged. Open access funding enabled and organized by Projekt DEAL.

Conflict of interest

The authors declare no conflict of interest.

Keywords: cascade · C–H activation · electrochemistry · oxygenation · rhodium

- [1] a) L. Woźniak, J.-F. Tan, Q.-H. Nguyen, A. Madron du Vigné, V. Smal, Y.-X. Cao, N. Cramer, *Chem. Rev.* **2020**, *120*, 10516–10543; b) S. Rej, Y. Ano, N. Chatani, *Chem. Rev.* **2020**, *120*, 1788–1887; c) P. Gandeepan, T. Müller, D. Zell, G. Cera, S. Warratz, L. Ackermann, *Chem. Rev.* **2019**, *119*, 2192–2452; d) Y. Park, Y. Kim, S. Chang, *Chem. Rev.* **2017**, *117*, 9247–9301; e) J. He, M. Wasa, K. S. L. Chan, Q. Shao, J.-Q. Yu, *Chem. Rev.* **2017**, *117*, 8754–8786; f) O. Daugulis, J. Roane, L. D. Tran, *Acc. Chem. Res.* **2015**, *48*, 1053–1064; g) J. Wencel-Delord, F. Glorius, *Nat. Chem.* **2013**, *5*, 369–375; h) B. Li, P. H. Dixneuf, *Chem. Soc. Rev.* **2013**, *42*, 5744–5767; i) D. A. Colby, A. S. Tsai, R. G. Bergman, J. A. Ellman, *Acc. Chem. Res.* **2012**, *45*, 814–825; j) L. McMurray, F. O'Hara, M. J. Gaunt, *Chem. Soc. Rev.* **2011**, *40*, 1885–1898; k) L. Ackermann, R. Vicente, A. R. Kapdi, *Angew. Chem. Int. Ed.* **2009**, *48*, 9792–9826; *Angew. Chem.* **2009**, *121*, 9976–10011.
- [2] a) D. Yasemin, O. Yasemin, O. Orhan, E. Volkan, O. Tijen, M. Adnan, E. Keveser, M. F. Sahin, *Med. Chem.* **2012**, *8*, 481–490; b) G. G. Duthie, A. D. Wood, *Food Funct.* **2011**, *2*, 515–520; c) D. Ekinci, M. Şentürk, Ö. İ. Küfrevioğlu, *Expert Opin. Ther. Pat.* **2011**, *21*, 1831–1841; d) Z. Rappoport, *The chemistry of phenols*, Wiley, Hoboken, **2004**.
- [3] a) S. De Sarkar, W. Liu, S. I. Kozhushkov, L. Ackermann, *Adv. Synth. Catal.* **2014**, *356*, 1461–1479; b) K. M. Engle, T.-S. Mei, M. Wasa, J.-Q. Yu, *Acc. Chem. Res.* **2012**, *45*, 788–802.
- [4] F. Mo, L. J. Trzepakowski, G. Dong, *Angew. Chem. Int. Ed.* **2012**, *51*, 13075–13079; *Angew. Chem.* **2012**, *124*, 13252–13256.
- [5] G. Shan, X. Yang, L. Ma, Y. Rao, *Angew. Chem. Int. Ed.* **2012**, *51*, 13070–13074; *Angew. Chem.* **2012**, *124*, 13247–13251.
- [6] a) Q. Bu, R. Kuniyil, Z. Shen, E. Gońka, L. Ackermann, *Chem. Eur. J.* **2020**, *26*, 16450–16454; b) G. G. Dias, T. Rogge, R. Kuniyil, C. Jacob, R. F. S. Menna-Barreto, E. N. da Silva Júnior, L. Ackermann, *Chem. Commun.* **2018**, *54*, 12840–12843; c) K. Raghuvanshi, D. Zell, L. Ackermann, *Org. Lett.* **2017**, *19*, 1278–1281; d) F. Yang, K. Rauch, K. Kettelhoit, L. Ackermann, *Angew. Chem. Int. Ed.* **2014**, *53*, 11285–11288; *Angew. Chem.* **2014**, *126*, 11467–11470; e) F. Yang, L. Ackermann, *Org. Lett.* **2013**, *15*, 718–720; f) W. Liu, L. Ackermann, *Org. Lett.* **2013**, *15*, 3484–3486; g) V. S. Thirunavukkarasu, J. Hubrich, L. Ackermann, *Org. Lett.* **2012**, *14*, 4210–4213; h) V. S. Thirunavukkarasu, L. Ackermann, *Org. Lett.* **2012**, *14*, 6206–6209.
- [7] a) Q. Gou, X. Tan, M. Zhang, M. Ran, T. Yuan, S. He, L. Zhou, T. Cao, F. Luo, *Org. Lett.* **2020**, *22*, 1966–1971; b) M. Bakthadoss, P. Vijay Kumar, R. Kumar, V. Agarwal, *Org. Biomol. Chem.* **2019**, *17*, 4465–4469; c) Z.-I. Li, K.-k. Sun, C. Cai, *Org. Chem. Front.* **2019**, *6*, 637–642; d) Y.-C. Yuan, C. Bruneau, V. Dorcet, T. Roisnel, R. Gramage-Doria, *J. Org. Chem.* **2019**, *84*, 1898–1907; e) Y.-C. Yuan, C. Bruneau, T. Roisnel, R. Gramage-Doria, *Org. Biomol. Chem.* **2019**, *17*, 7517–7525; f) C. Chen, Y. Pan, H. Zhao, X. Xu, J. Xu, Z. Zhang, S. Xi, L. Xu, H. Li, *Org. Chem. Front.* **2018**, *5*, 415–422; g) A. Mishra, T. K. Vats, M. P. Nair, A. Das, I. Deb, *J. Org. Chem.* **2017**, *82*, 12406–12415; h) Y. Wu, B. Zhou, *Org. Lett.* **2017**, *19*, 3532–3535; i) T. H. L. Nguyen, N. Gigant, S. Delarue-Cochin, D. Joseph, *J. Org. Chem.* **2016**, *81*, 1850–1857; j) Y.-H. Sun, T.-Y. Sun, Y.-D. Wu, X. Zhang, Y. Rao, *Chem. Sci.* **2016**, *7*, 2229–2238; k) H. Batchu, S. Bhattacharyya, R. Kant, S. Batra, *J. Org. Chem.* **2015**, *80*, 7360–7374; l) K. Kim, H. Choe, Y. Jeong, J. H. Lee, S. Hong, *Org. Lett.* **2015**, *17*, 2550–2553; m) G. Li, L. Wan, G. Zhang, D. Leow, J. Spangler, J.-Q. Yu, *J. Am. Chem. Soc.* **2015**, *137*, 4391–4397; n) Y.-F. Liang, X. Wang, Y. Yuan, Y. Liang, X. Li, N. Jiao, *ACS Catal.* **2015**, *5*, 6148–6152; o) G. Shan, X. Han, Y. Lin, S. Yu, Y. Rao, *Org. Biomol. Chem.* **2013**, *11*, 2318–2322; p) P. Y. Choy, F. Y. Kwong, *Org. Lett.* **2013**, *15*, 270–273; q) H.-Y. Zhang, H.-M. Yi, G.-W. Wang, B. Yang, S.-D. Yang, *Org. Lett.* **2013**, *15*, 6186–6189.
- [8] a) K. Yamamoto, M. Kuriyama, O. Onomura, *Acc. Chem. Res.* **2020**, *53*, 105–120; b) F. Wang, S. S. Stahl, *Acc. Chem. Res.* **2020**, *53*, 561–574; c) J. C. Siu, N. Fu, S. Lin, *Acc. Chem. Res.* **2020**, *53*, 547–560; d) J. L. Röckl, D. Pollok, R. Franke, S. R. Waldvogel, *Acc. Chem. Res.* **2020**, *53*, 45–61; e) Q. Jing, K. D. Moeller, *Acc. Chem. Res.* **2020**, *53*, 135–143; f) K.-J. Jiao, Y.-K. Xing, Q.-L. Yang, H. Qiu, T.-S. Mei, *Acc. Chem. Res.* **2020**, *53*, 300–310; g) L. Geske, E. Sato, T. Opatz, *Synthesis* **2020**, *52*, 2781–2794; h) T. Fuchigami, S. Inagi, *Acc. Chem. Res.* **2020**, *53*, 322–334; i) Y. Yuan, A. Lei, *Acc. Chem. Res.* **2019**, *52*, 3309–3324; j) P. Xiong, H.-C. Xu, *Acc. Chem. Res.* **2019**, *52*, 3339–3350; k) M. Elsherbini, T. Wirth, *Acc. Chem. Res.* **2019**, *52*, 3287–3296; l) S. R. Waldvogel, S. Lips, M. Selt, B. Riehl, C. J. Kampf, *Chem. Rev.* **2018**, *118*, 6706–6765; m) M. Yan, Y. Kawamata, P. S. Baran, *Chem. Rev.* **2017**, *117*, 13230–13319; n) R. Feng, J. A. Smith, K. D. Moeller, *Acc. Chem. Res.* **2017**, *50*, 2346–2352; o) R. Francke, R. D. Little, *Chem. Soc. Rev.* **2014**, *43*, 2492–2521; p) A. Jutand, *Chem. Rev.* **2008**, *108*, 2300–2347.
- [9] a) P. Gandeepan, L. H. Finger, T. H. Meyer, L. Ackermann, *Chem. Soc. Rev.* **2020**, *49*, 4254–4272; b) T. H. Meyer, I. Choi, C. Tian, L. Ackermann, *Chem* **2020**, *6*, 2484–2496; c) H. Wang, X. Gao, Z. Lv, T. Abdelilah, A. Lei, *Chem. Rev.* **2019**, *119*, 6769–6787; d) T. H. Meyer, L. H. Finger, P. Gandeepan, L. Ackermann, *Trends Chem.* **2019**, *1*, 63–76; e) Q.-L. Yang, P. Fang, T.-S. Mei, *Chin. J. Chem.* **2018**, *36*, 338–352; f) C. Ma, P. Fang, T.-S. Mei, *ACS Catal.* **2018**, *8*, 7179–7189; g) N. Sauermann, T. H. Meyer, Y. Qiu, L. Ackermann, *ACS Catal.* **2018**, *8*, 7086–7103.
- [10] a) L. Massignan, X. Tan, T. H. Meyer, R. Kuniyil, A. M. Messinis, L. Ackermann, *Angew. Chem. Int. Ed.* **2020**, *59*, 3184–3189; *Angew. Chem.* **2020**, *132*, 3210–3215; b) S.-K. Zhang, J. Struwe, L. Hu, L. Ackermann, *Angew. Chem. Int. Ed.* **2020**, *59*, 3178–3183; *Angew. Chem.* **2020**, *132*, 3204–3209; c) T. H. Meyer, J. C. A. Oliveira, D. Ghorai, L. Ackermann, *Angew. Chem. Int. Ed.* **2020**, *59*, 10955–10960; *Angew. Chem.* **2020**, *132*, 11048–11053; d) C. Tian, U. Dhawa, J. Struwe, L. Ackermann, *Chin. J. Chem.* **2019**, *37*, 552–556; e) A. Shrestha, M. Lee, A. L. Dunn, M. S. Sanford, *Org. Lett.* **2018**, *20*, 204–207; f) Q.-L. Yang, Y.-Q. Li, C. Ma, P. Fang, X.-J. Zhang, T.-S. Mei, *J. Am. Chem. Soc.* **2017**, *139*, 3293–3298; g) Y.-Q. Li, Q.-L. Yang, P. Fang, T.-S. Mei, D. Zhang, *Org. Lett.* **2017**, *19*, 2905–2908; h) N. Sauermann, T. H. Meyer, C. Tian, L. Ackermann, *J. Am. Chem. Soc.* **2017**, *139*, 18452–18455.
- [11] a) L. Ackermann, *Acc. Chem. Res.* **2020**, *53*, 84–104; b) Y. Qiu, J. Struwe, L. Ackermann, *Synlett* **2019**, *30*, 1164–1173.
- [12] a) A. Modak, U. Dutta, R. Kancherla, S. Maity, M. Bhadra, S. M. Mobin, D. Maiti, *Org. Lett.* **2014**, *16*, 2602–2605; b) R. Mueller, S. Rachwal, M. E. Tedder, Y.-X. Li, S. Zhong, A. Hampson, J. Ulas, M. Varney, L. Nielsson, G. Rogers, *Bioorg. Med. Chem. Lett.* **2011**, *21*, 3927–3930; c) G. R. Madhavan, R. Chakrabarti, K. Anantha Reddy, B. M. Rajesh, V. Balraju, P. Bheema Rao, R. Rajagopalan, J. Iqbal, *Bioorg. Med. Chem.* **2006**, *14*, 584–591.
- [13] For detailed information, see the Supporting Information.
- [14] L. E. Shmukler, M. S. Gruzdev, N. O. Kudryakova, Y. A. Fadeeva, A. M. Kolker, L. P. Safonova, *RSC Adv.* **2016**, *6*, 109664–109671.

- [15] a) C. E. Keohane, A. D. Steele, C. Fetzer, J. Khowsathit, D. Van Tyne, L. Moynié, M. S. Gilmore, J. Karanicolas, S. A. Sieber, W. M. Wuest, *J. Am. Chem. Soc.* **2018**, *140*, 1774–1782; b) A. D. Steele, C. E. Keohane, K. W. Knouse, S. E. Rossiter, S. J. Williams, W. M. Wuest, *J. Am. Chem. Soc.* **2016**, *138*, 5833–5836; c) A. D. Steele, K. W. Knouse, C. E. Keohane, W. M. Wuest, *J. Am. Chem. Soc.* **2015**, *137*, 7314–7317; d) W. Li, P. Estrada-de los Santos, S. Matthijs, G.-L. Xie, R. Busson, P. Cornelis, J. Rozenski, R. De Mot, *Chem. Biol.* **2011**, *18*, 1320–1330.

Manuscript received: December 31, 2020

Revised manuscript received: February 28, 2021

Accepted manuscript online: March 2, 2021

Version of record online: May 7, 2021